Highlighting the research collaboration between Dr John Younger of the Department of Emergency Medicine and Dr Michael Solomon (2011 Soft Matter Lectureship winner) of the Department of Chemical Engineering at the University of Michigan, USA.

Title: *In situ* rheology of *Staphylococcus epidermidis* bacterial biofilms

This work reports the adaptation of a parallel plate rheometer to function as a continuously fed bioreactor, thereby allowing characterization of the mechanical properties of bacterial biofilms grown under conditions of controlled growth media, temperature, and shear.

RSCPublishing

www.rsc.org/softmatter

PAPER

In situ rheology of *Staphylococcus epidermidis* bacterial biofilms

Leonid Pavlovsky,[a] John G. Younger*[bcd] and Michael J. Solomon*[ac]

We developed a method to grow *Staphylococcus epidermidis* bacterial biofilms and characterize their rheological properties *in situ* in a continuously fed bioreactor incorporated into a parallel plate rheometer. The temperature and shear rates of growth modeled bloodstream conditions, a common site of *S. epidermidis* infection. We measured the linear elastic (G') and viscous moduli (G'') of the material using small-amplitude oscillatory rheology and the yield stress using non-linear creep rheology. We found that the elastic and viscous moduli of the *S. epidermidis* biofilm were 11 ± 3 Pa and 1.9 ± 0.5 Pa at a frequency of 1 Hz (6.283 rad per s) and that the yield stress was approximately 20 Pa. We modeled the linear creep response of the biofilm using a Jeffreys model and found that *S. epidermidis* has a characteristic relaxation time of approximately 750 seconds and a linear creep viscosity of 3000 Pa s. The effects on the linear viscoelastic moduli of environmental stressors, such as NaCl concentration and extremes of temperature, were also studied. We found a non-monotonic relationship between moduli and NaCl concentrations, with the stiffest material properties found at human physiological concentrations (135 mM). Temperature dependent rheology showed hysteresis in the moduli when heated and cooled between 5 °C and 60 °C. Through these experiments, we demonstrated that biofilms are rheologically complex materials that can be characterized by a combination of low modulus ($\sim$10 Pa), long relaxation time ($\sim$10^3 seconds), and a finite yield stress (20 Pa). This suggests that biofilms should be viewed as soft viscoelastic solids whose properties are determined in part by local environmental conditions. The *in situ* growth method introduced here can be adapted to a wide range of biofilm systems and applied over a broad spectrum of rheological and environmental conditions because the technique minimizes the risk of irreversible, non-linear deformation of the microbial specimen before analysis.

Introduction

Bacterial biofilms are matrix-enclosed multicellular communities of microorganisms that can colonize environmental and man-made surfaces of ecological, industrial, and medical significance.[1–4] In most bacterial biofilms, the matrix is comprised primarily of a bacterially synthesized extracellular polymeric substance (EPS) that acts as a protective barrier. The EPS improves bacterial fitness through a set of mechanisms that are thought to include resistance to the diffusion of antimicrobial agents, promotion of intercellular communication to induce more resilient patterns of gene expression, and reversible deformation to resist fragmentation due to applied stresses.[1,2,5,6] The EPS is composed partially of protein and DNA, but predominantly of polysaccharides.[5,7]

Biofilms are persistent in a variety of settings where knowledge of their mechanical properties would be useful to maintaining clean surfaces as well as preserving the efficiency and effectiveness of the fouled components. For example, biofilm species can grow on the hulls of ships, increasing drag and overall fuel consumption for transportation.[8] Similarly, a buildup of biofilm in industrial pipelines can cause a loss of hydrodynamic pressure, leading to increased power consumption, decreased plant efficiency, as well as possible cooling failures.[9] Importantly, biofilms also colonize implanted medical devices in concentrated regions, which tend to fragment under the shear stresses of blood and disseminate bacteria through the bloodstream, causing infection.[2]

A biofilm-forming species of particular interest to human health is *Staphylococcus epidermidis*. *S. epidermidis* is a normal member of skin flora. Commonly, this organism infects patients by contaminating the surface of medical devices at the time of surgical implantation or subsequently during routine care of such devices.[10] Although not generally severe,

[a]*Department of Chemical Engineering, University of Michigan, Ann Arbor, MI, 48109, USA. E-mail: mjsolo@umich.edu; Fax: +1 734 763 0459; Tel: +1 734 764 3119*

[b]*Department of Emergency Medicine, University of Michigan, Ann Arbor, MI, 48109, USA. E-mail: jyounger@umich.edu; Tel: +1 734 647 7564*

[c]*Biointerfaces Institute, University of Michigan, Ann Arbor, MI, 48109, USA*

[d]*Michigan Center for Integrative Research in Critical Care, University of Michigan, Ann Arbor, MI, 48109, USA*

S. epidermidis infections have a mortality rate above 30% in a population of immunocompromised patients.[10,11] Much more commonly, *S. epidermidis* biofilm formation prompts surgical removal and replacement of the affected implanted device, with the associated costs and risks of that procedure.[6]

Many implanted devices susceptible to colonization by this organism are positioned in the bloodstream, such as intravenous and intraarterial catheters, dialysis catheters, and prosthetic heart valves. In this setting, *S. epidermidis* biofilm extent and structure reflects immunological and physical interactions with the host, including hydrodynamic forces imposed by flowing blood in particular.[12] Accordingly, reducing the disease burden associated with *S. epidermidis* may require better understanding of the mechanical features that allow it to persist in the bloodstream.

Biofilms must be cultivated prior to rheological characterization. As a result, rheological measurements typically follow one of two paths: In the first, a biofilm is cultivated in a bioreactor, and then physically transferred to the rheometer for characterization. In the second, the rheological evaluation is performed *in situ*, but perhaps limited or non-standard techniques are used. Examples in literature of the former include samples scraped off of their growth environment by Shaw *et al.*, and samples grown on suspended rheometer plates connected to a drive shaft and then moved to the analytical device by Towler *et al.* An example of the latter includes observations of biofilms grown on a microfluidic device by Hohne *et al.*[1,13,14] Other biofilm rheology studies have been reviewed by Wilking *et al.*[15]

Evidence for divergent results from these two approaches can be found in the broad range of values for the linear elastic modulus that have been reported in the literature for *S. epidermidis* biofilms, which include those of Di Stefano *et al.* (0.5 kPa), Jones *et al.* (0.5–15 kPa), Hohne *et al.* (3.2 kPa), and Aggarwal *et al.* (0.1–8.0 kPa).[13,16–19] There is little doubt that biofilm mechanics are dependent on the conditions under which they develop.[20] It appears that the challenges posed by evaluating biofilms *in situ* in current rheometric fixtures have produced considerable uncertainty in biofilm mechanical properties reported in the literature. Experimental measurements that address the challenge of *in situ* growth and evaluation can support the development of theoretical models for biofilm mechanics that are grounded in polysaccharide and polymer rheology. They can furthermore be applied to evaluate hypotheses about the interaction of biofilms with the hydrodynamic stresses generated in the circulatory system.

Here we address the need for an *in situ* rheological characterization method for cultured biofilms. The method uses a chamber for *in situ* growth of biofilms under the fixture of a standard rheometer. After an initial phase of growth, the biofilm is fused to the rheometer fixture, thereby allowing rheological characterization of the bacterial biofilms. This method, here applied to the particular case of *S. epidermidis* biofilms, transforms a parallel plate rheometer into a continuously fed bacterial bioreactor, thereby allowing the *in situ* rheological characterization to proceed. By doing so, we were able to sequentially grow biofilms under defined shear forces and then perform small-amplitude oscillatory rheology and non-linear creep rheology, without disrupting the test material from its original site of growth. With this method, we report the characterization of the viscoelastic properties of *S. epidermidis* biofilms. We explore the impact on mechanical behavior of a well-known metabolic stressor, osmotic stress, which is generated by growth under high salt conditions. Additionally, we observe the behavior of biofilm mechanical properties under a range of temperatures and find behavior that reveals that complex rheology of these multiphase materials.

Methods and materials

Staphylococcus epidermidis

S. epidermidis of strain RP62A, a biofilm-forming clinical isolate was obtained from American Type Culture Collection (culture 35984) and grown in tryptic soy broth (TSB; Fluka Scientific) media supplemented with 1% D-(+)-glucose (Sigma Life Science, 86 mM NaCl, viscosity 0.88 Pa s at 37 °C). For experiments probing the osmotic stress induced by sodium chloride, media were enriched to 135 mM NaCl – which is reflective of human blood stream salinity, or 770 mM NaCl – the conventional high-stress condition used in the literature.[21,22] As the rheometer bioreactor is an open system and therefore prone to contamination, cycloheximide (90 μg mL^{-1}; Fluka Scientific) and kanamycin (50 μg mL^{-1}; Sigma-Aldrich) were used as an antifungal and general antibacterial, respectively.[23,24] The impact of both was confirmed in preliminary experiments in which *S. epidermidis* was cultured on tryptic soy agar plates in which each compound had been dosed. Neither had any discernible effect on *S. epidermidis* growth by a count of colony-forming units.

Rheometry

A mechanical rheometer (TA Instruments AR-G2) was used to create a controlled-shear rate environment during growth and characterization of the biofilm. The geometry used was a 40 mm stainless steel parallel plate. We conducted growth and testing while the geometry was submerged in media at gap heights between 250 μm and 1 mm. The lower limit was chosen because it was the minimal gap height for instrument sensitivity, as determined through independent testing on aqueous solutions of poly(ethylene oxide). This configuration was made possible by the use of an immersion ring attached to the bottom Peltier plate of the rheometer, which acted to keep the parallel plate geometry submerged in TSB media (Fig. 1). The novelty of this approach is that it allows the biofilm to grow under the rheometer fixture as the media is slowly convected over the growth area while, simultaneously, the level is controlled.

To sterilize the apparatus prior to experiments, we filled the immersion bath with ethanol, and allowed it to disinfect for approximately 30 minutes. Additionally, we used a custom-made plastic cover to reduce the opportunity for airborne contamination of the open reactor. Variable-flow peristaltic pumps (Fisher Scientific) were used to constantly replenish the media in a chemostat configuration at a rate of approximately 0.5 mL min^{-1} with a total fill volume of approximately 30 mL,
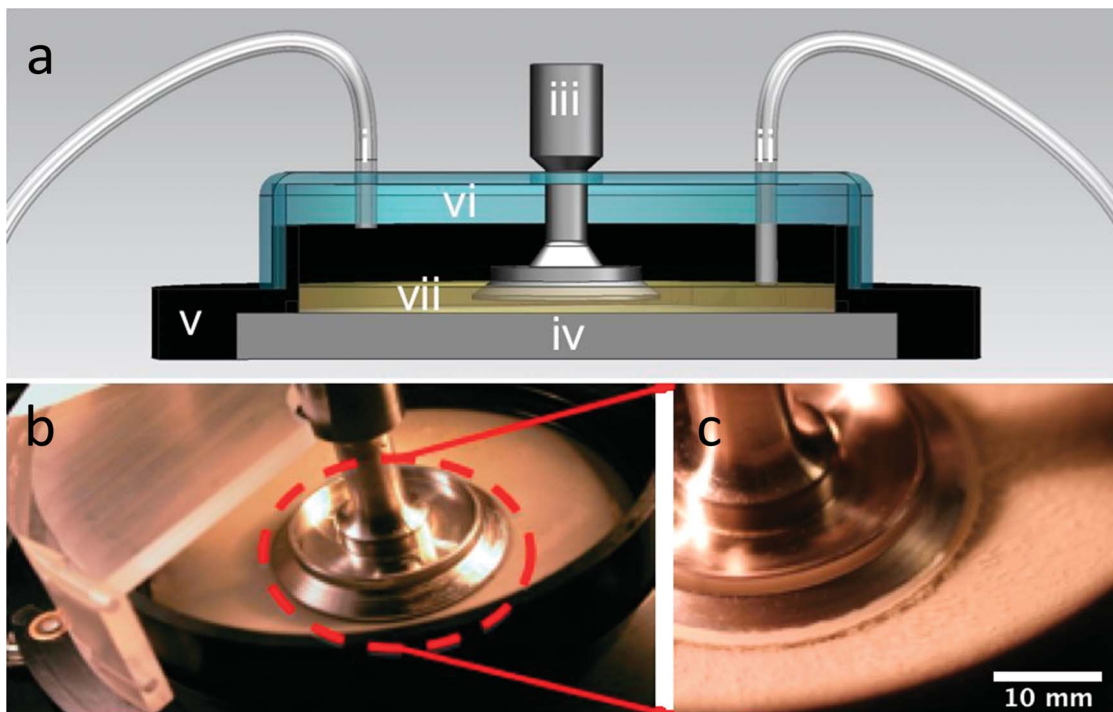
Fig. 1 (a) Cross-sectional schematic of continuously fed rheometer bacterial bioreactor where (i) is the growth media inlet, (ii) is the outlet, (iii) is the rheometer fixture, (iv) is the Peltier plate for temperature control, (v) is the immersion ring, (vi) is the cover, and (vii) is the liquid growth media, which is maintained at a fixed level by the outlet suction. (b) Overhead view of the open rheometer bioreactor. (c) Close-up view of the rheometer geometry of the bioreactor with *Staphylococcus epidermidis* biofilms grown, post-analysis.

giving a media turnover rate of approximately 1 h^{-1}. After reaching fill volume, we inoculated the media within the immersion ring with 2 mL of the initial *S. epidermidis* culture by pipette.

The experimental protocol is divided into three phases: growth, attachment, and rheological characterization. All phases of the experiments were conducted at 37 °C unless otherwise noted.

1 GROWTH. During the growth phase, the rheometer parallel plate was positioned at a gap of 1.0 mm. Within the human circulatory system, which is a common contamination site for such biofilms, the shear rate can be in excess of 100 s^{-1} and the shear stress is in the range of 0.076–0.76 Pa.[21,25] Therefore, we rotate the plate to generate an initial shear stress of 0.1 Pa, which corresponds to a shear rate of 113.6 s^{-1}. This shear rate is held fixed during the growth phase. Biochemical assessment of the reactor in the opening hours of the growth phase confirmed a transition from aerobic to micro-aerobic growth as oxygen and glucose consumption fell to steady-state values within 7 hours. Altogether, growth was allowed to continue for 17 hours, after which the gap was reduced to 300 μm. This reduction in gap allowed the biofilm cultured on the base to come in contact with the upper plate. This timescale for growth was chosen due to the constraints of the organism and our interests in analysis, and could be varied to suit differences in organism and environment. At the conclusion of the growth phase, the biofilm has covered the rheometer Peltier plate completely, but has yet to connect to the upper plate.

2 ATTACHMENT. The attachment phase was a 7-hour period of linear oscillation of the geometry that allowed the biofilm to fuse from the rheometer Peltier plate to the upper plate. We accomplished this by reducing the parallel plate gap height to 300 μm and oscillating the plate at a strain of 0.016 for 7 hours. An oscillatory study at various gap heights was conducted to determine the maximum allowable gap height. The oscillatory strain of 0.016 was chosen such that it was within the linear viscoelastic regime of the biofilm to avoid altering the material before testing. We chose the 7-hour period because it provided for sufficient growth of the biofilm, as was discussed in the previous section.

We established a criterion to systematically determine whether a sample had attached to both the top and bottom of the parallel plate rheometer fixture, and thus was a good candidate for further rheological testing. During attachment, the linear elastic and viscous moduli, G' and G'', respectively, were measured over time. Only biofilms whose moduli reached steady-state by the end of the 7-hour period were judged to have attached. The rate for successful attachment was approximately 70%. Examples of the time-dependent elastic modulus for attached and unattached biofilms are shown in Fig. 2; distinguishing between the two cases was straightforward because of the large rheological differences between the two states.

In addition to the attachment criterion, we performed three other studies to evaluate the quality of the rheological measurements on the biofilm. First, we evaluated the overall biofilm coverage. We removed the geometry fixture after
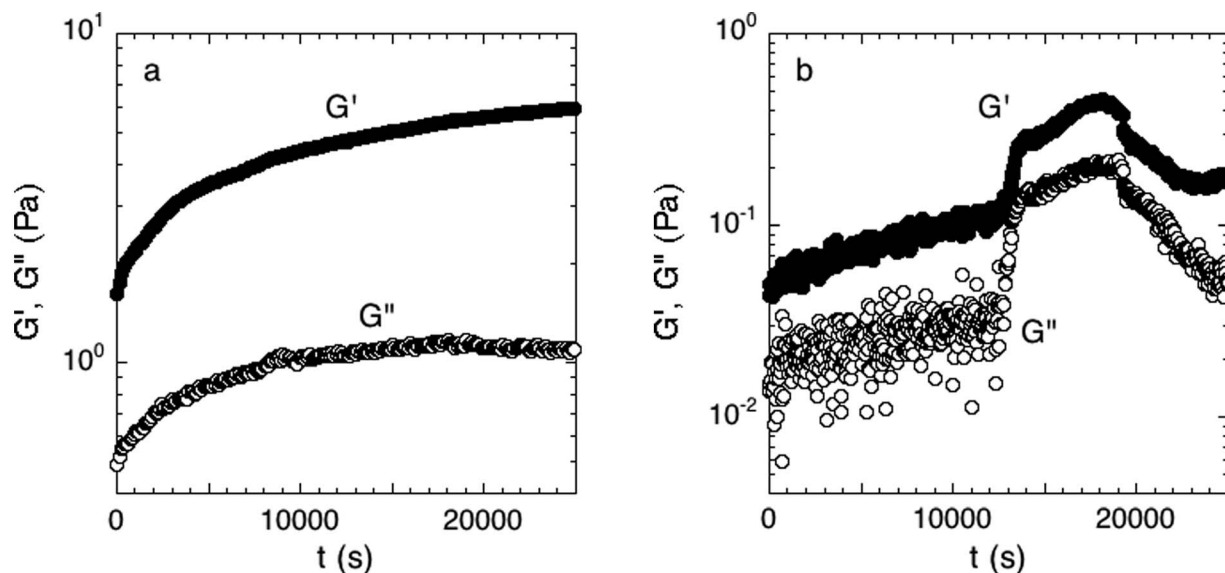
Fig. 2 (a) Accepted and (b) rejected attachment phase. Measured over 7 hours at 300 μm and a strain of 0.016 directly after the initial growth period. The moduli in the accepted experiment have reached equilibrium while the rejected experiment has not. Examples of one experiment of each case are shown.

rheological measurements were completed, stained the bacterial cells with Gram crystal violet (Becton, Dickinson and Company), and rinsed off the excess. In all attached samples, biofilm coverage was equal to or greater than 95% of the analytical surface area of the geometry. Second, we stained and imaged biofilm sampled from a number of regions of the rheometer with confocal laser scanning microscopy (CLSM) as per the methods of Hohne *et al.* and Dzul *et al.*[13,26] These images showed that the biofilms displayed a uniform microscopic morphology over the testing surface. Representative images of the Gram staining and confocal microscopy are reported in Fig. 3. Third, we evaluated the effect of parallel plate diameter on the rheology. In this testing, we applied the same growth and attachment procedures for a 60 mm parallel plate geometry. For the case of no added NaCl, the measured G' and G'' did not show a significant difference between tests conducted with a 40 mm and 60 mm; measurements at all frequencies were within one standard deviation. This result demonstrates geometry independence of the material properties of the tested biofilms. A final issue was the selection between parallel plate fixtures and the cone and plate geometry for measurements. We opted for the former because of the nonhomogeneous nature of the biofilms, the need to assess the effect of multiple gap heights and pre- and post-compression testing, and because of the performance of temperature dependence rheology.

3 RHEOLOGICAL CHARACTERIZATION

a) Small-amplitude oscillatory rheology. After the attachment phase, we determined the linear viscoelasticity of the biofilm by small-amplitude oscillatory deformation over the frequency range of 0.005–10 Hz (0.0314–62.83 rad per s) and strain amplitude of 0.13 (approximately 10% of the maximum strain within the linear viscoelastic limit). The measurements were conducted at gap heights of 300 and 250 μm, under compression and tension. The variation in gap was used to check for hysteresis in gap height.

b) Creep rheology. We measured the creep compliance, $J(t, \sigma_o)$, of a number of specimens to extend the regime of linear rheological characterization to long times (low frequencies) and to determine the non-linear rheological response of the biofilms, including their yield stress. These tests were performed immediately after the small-amplitude oscillatory rheology measurements. The experiments were conducted for duration of 20 minutes. The measurements were performed at the following applied stresses: 0.1 Pa, 0.2 Pa, 0.5 Pa, 1.0 Pa, and then up to 100 Pa in increments of 5 Pa.

c) Temperature dependent rheology. The effect of temperature on the linear viscoelasticity of the biofilms was studied by means of small-amplitude oscillatory rheology. Initial tests on attached biofilms were conducted at 37 °C. Then, the specimen temperature was decreased to 5 °C and linear viscoelasticity measured. This procedure was repeated at temperatures from 5 °C to 60 °C in increments of 5 °C. To evaluate hysteresis, measurements were then performed from 60 °C to 10 °C, with temperature decreased in increments of 5 °C. Temperature changes were rapidly induced by the Peltier component of the rheometer.

Sensitivity analysis of small-amplitude rheology

We found that bacterial biofilms displayed greater specimen-to-specimen variability in their rheology than synthetic materials, such as polymer melts or colloidal suspensions. To address this variability, we performed statistical analyses standard in the biological sciences to evaluate for differences in rheology between different biofilm growth conditions. To examine the impact of such experimental conditions on the G'-frequency and G''-frequency relationships, a linear mixed effects regression approach was used as implemented in the *lme* function in the statistical package R 2.13.2. Frequency, NaCl concentration, the gap height, and whether measurements were taken before

Fig. 3 (a) Base of rheometer immediately after draining media and lifting the parallel plate. (b) 40 mm diameter parallel plate stained with Gram crystal violet depicting full coverage of biofilm. (c and d) CLSM images of various areas of the biofilm after rheological testing, showing similar morphology throughout.

or after a compressive strain were considered as fixed effects. Individual biofilms were considered as a random effect. For analysis of G', modeling was performed with log transforms of G' and angular frequency. For G'', similar modeling was performed but included also polynomial fitting of the G''-frequency curve. Between-model comparisons were performed using *anova.lme* in the same package.

Results and discussion

Small-amplitude oscillatory rheology of *S. epidermidis*

Small-amplitude oscillatory rheology was used to determine the frequency dependence of the elastic and viscous moduli of *S. epidermidis* biofilms (Fig. 4). The elastic modulus, G', was approximately 10 Pa and exhibited a power-law increase at increasing angular frequency while the viscous modulus, G'', was on the order of 1 Pa and deviated from power-law behavior at increasing angular frequency. For comparison, soft living tissues have the following elastic moduli: swine brain (260–490 Pa), human liver (640 Pa), human breast tumor (4 kPa), rat

skeletal muscle (100 kPa), and bovine cartilage (950 kPa).[27–31] As G' is greater than G'' at all frequencies studied, the material is elastic and solid-like. Unfortunately, due to the small frequency range, and the lack of applicability of time–temperature superposition (as discussed in a later section), this technique does not reveal much about the material rheology other than confirming that biofilms are soft, viscoelastic materials. The non-linear rheological characterization by creep will provide a better indication of the mechanical properties of the biofilm. We can, however, conclude from the linear rheology that the longest viscoelastic relaxation time of the biofilm must be greater than $\sim 10^2$ seconds because no terminal region was observed within the frequency range of the measurements. This conclusion is consistent with the findings of Shaw *et al.* for the case of *S. aureus*, *Pseudomonas aeruginosa*, and natural pond biofilms.[1]

More specifically, the *S. epidermidis* elastic and viscous moduli resemble those of soft glassy materials at frequencies above the onset of the plateau region and at temperatures below the glass transition.[32] At that point, the elastic modulus exhibits the same
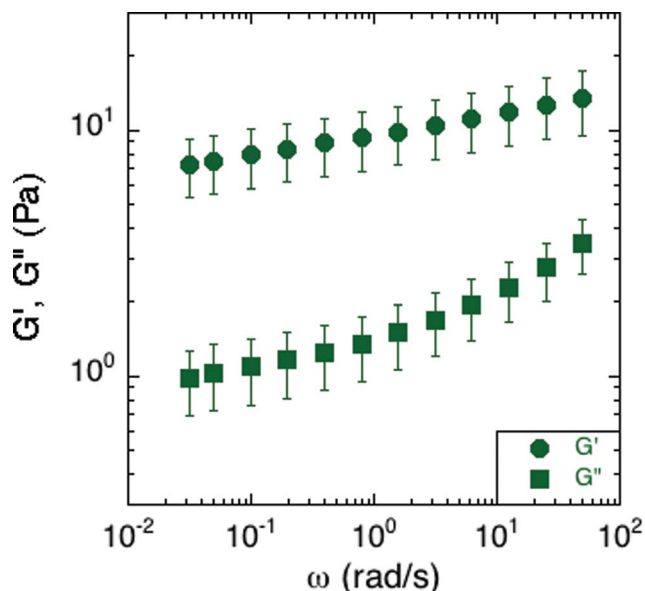
Fig. 4 Elastic and viscous moduli of *S. epidermidis* biofilms grown in TSB with 86 mM NaCl. This data includes 6 replicates, with each comprised of an average modulus of the experiments conducted at 300 and 250 μm under both compression and tension. Error bars represent the standard error of the mean.

Fig. 5 Creep of *S. epidermidis* grown in TSB with 86 mM NaCl. A constant stress was applied at $t = 0$ and the material compliance measured over 20 minutes. Data shown from 1 experiment for purposes of clarity.

power-law increase as that of the biofilm while the viscous modulus exhibits a greater rate of increase after passing a local minimum. Other soft glassy materials with analogous properties include jammed emulsions, colloidal glasses and colloidal gels.[33–35]

However, as compared to previous findings, the moduli from the small-amplitude rheology of *S. epidermidis* are at least an order of magnitude less than previously reported for *S. epidermidis* biofilms.[13,16–19] A possible origin of this large variability could be the sensitivity of biofilm elasticity to measurement strategies and environmental conditions. For example, measurements conducted under shear deformation instead of tensile deformation can result in properties for gels and pastes that vary by a factor of 50.[36] Moreover, the *in situ* growth protocol could also play a role: By providing a continuous source of nutrients and fluids, as is present in the natural environment of *S. epidermidis*, mechanical properties potentially avoid a regime of extremely high moduli more commonly seen in a dry-growth environment. (Recall that biofilms themselves are ∼80% water, so properties could be very sensitive to degree of hydration[37]) Additionally, in this work, by removing the need to transport the biofilm, we avoid the risk of altering or compacting it. Such a transport step could lead to a collapse of the microstructure of water channels known to exist in biofilms, and thereby increase the overall concentration of cells and polymer per volume of the biofilm and with it, the modulus.[38,39]

Creep compliance of *S. epidermidis*

To study the non-linear rheology of the *S. epidermidis* biofilms, the creep compliance of the biofilm was measured as a function of time (Fig. 5). A number of interesting features of the creep compliance are apparent from this measurement.
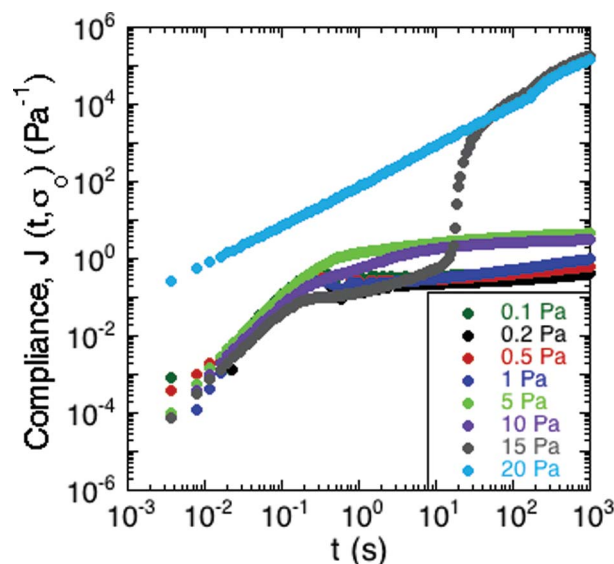
First, at low applied stress, there is a region of linear viscoelastic behavior. The compliance displayed a nearly instantaneous step response followed by a plateau region and then a small, progressive increase in compliance at long times. These observations are consistent with the behavior of a viscoelastic solid with long-term creep.
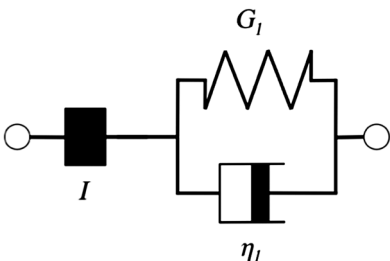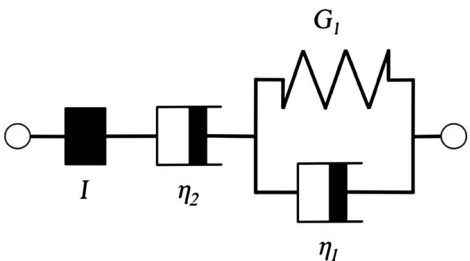
Second, a transition from solid- to liquid-like behavior is evident in the graph at 15 Pa of applied stress. At the intermediate stress of 15 Pa, there is an upturn after the instantaneous step response, which illustrates a transition from solid-like deformation to viscous-like flow in the material.

Third, at applied stresses above 15 Pa, the creep compliance increased linearly as a function of time, as is characteristic of a viscous liquid with a viscosity of approximately 8.3 mPa s.

The behavior in Fig. 5 is consistent with a soft glassy rheological response for the biofilm, as has been reported for gels, pastes and nanocomposites.[40–42] The solid regime is characterized by a finite compliance being achieved at relatively low applied stresses, followed by very slow creep indicative of a very high viscosity. Upon greater applied stresses, this critical deformation is surpassed and the material flows like a liquid. The transition is consistent with a yield stress for the biofilm.[41] Although this value varies from sample to sample, Fig. 5 illustrates the characteristic trend that was observed. This generic behavior has previously been reported in gels of polymers and pastes of particle suspensions.[40] The average yield stress of the 3 samples was approximately 20 Pa.

Additionally, we characterized the creep compliance response through modeling. In previous work, Towler *et al.* fit a linear viscoelastic Burgers model for the creep-stress relaxation spectrum of a mixed culture of biofilms.[14] We fit the *S. epidermidis* biofilms with three different viscoelastic solid models to capture the linear behavior of the material prior to yielding: the Burgers model, the Kelvin–Voigt model, and the

Table 1 Viscoelastic Kelvin–Voigt and Jeffreys models and their corresponding mathematical equations composed of springs (G_1), dashpots (η_1 and η_2), and inertial terms (I) that were used to capture the linear creep behavior of *S. epidermidis*. The values of the parameters determined to be a good fit by visual inspection are listed. The models were adapted from Ewoldt and McKinley, and Baravian and Quemada (ref. 43 and 44)[a]

Kelvin–Voigt	Jeffreys

Kelvin–Voigt:

$$J(t,\sigma_o) = \frac{1}{G_1}\left\{1 - e^{-At}\left[\cos(\omega t) + \frac{A}{\omega}\sin(\omega t)\right]\right\}$$

$$A = \frac{\eta_1 b}{2I} \qquad \omega = \sqrt{\frac{G_1 b}{I} - A^2}$$

$G_1 = 5.2$ Pa $\eta_1 = 0.095$ Pa s

Jeffreys:

$$J(t,\sigma_o) = \frac{t}{\eta_2} - B + e^{-At}\left\{B\cos(\omega t) + \frac{A}{\omega}\left[B - \frac{1}{\eta_2 A}\right]\sin(\omega t)\right\}$$

$$A = \frac{G_1 + \eta_1\eta_2 b/I}{2(\eta_1 + \eta_2)} \qquad B = \frac{\eta_1 + \eta_2}{G_1\eta_2}\left(\frac{2AI}{\eta_2 b} - 1\right) \qquad \omega = \sqrt{\frac{G_1 b}{I}\frac{\eta_2}{(\eta_1 + \eta_2)} - A^2}$$

$G_1 = 4.0$ Pa $\eta_1 = 0.095$ Pa s $\eta_2 = 3000$ Pa s

[a] $I = I_{\text{instrument}} + I_{\text{geometry}}$, b (cone and plate) $= 2\pi R^3/(3\tan\theta)$, b (parallel plate) $= \pi R^4/(2h)$.

Jeffreys model.[14,43–45] In order to capture the short-time behavior and creep ringing seen in our experiments, an inertial term was required for each model. This inertial term represents the inertia of the mobile part of the apparatus, which in our case is the rheometer spindle and the parallel plate geometry.[44] We found that the additional complexity in the Burgers model of a finite jump to compliance was not needed, therefore we only modeled the linear creep data with the Kelvin–Voigt and Jeffreys models. These models and their respective equations can be seen in Table 1.

Both the Kelvin–Voigt and the Jeffreys models incorporate a short-time viscosity (η_1), an elastic modulus (G_1), and an inertial term (I). The difference between these models lies in the

Fig. 6 Linear region of creep of *S. epidermidis* (stress of 0.1–1 Pa) fit with Kelvin–Voigt and Jeffreys models. The error bars are standard error of the mean.

addition of a linear creep viscosity (η_2) in the Jeffreys model. The reported fit parameters (η_1, η_2, and G_1) for both models generate a good agreement between the models and the data, as is apparent by inspection of Fig. 6. As seen in that figure, the lack of a linear creep viscosity term in the Kelvin–Voigt model does not allow it to capture the long-time behavior of the material; thus the Jeffreys model is preferred for modeling the linear viscoelasticity of the *S. epidermidis* biofilms.

Thus, the Jeffreys model successfully predicts the creep response of the *S. epidermidis* biofilm in all of previously described regions. In optimizing the Jeffreys model, we noticed that the η_1 term accounts for the magnitude of the creep ringing, the η_2 term dictates the long-term creep viscosity, and the G_1 term is responsible for the overall magnitude of the compliance. The viscous terms were found to be approximately 0.095 Pa s and 3000 Pa s for η_1 and η_2, respectively. This is particularly interesting when compared to the viscosity of 8.3 mPa s after the biofilm yields. The comparison shows how significantly the material is affected by the imposed stress and how viscous the material is at long times. The modulus was found to be approximately 4 Pa. The relaxation times of the biofilm are approximately 750 seconds, and were calculated as follows: $\lambda_1 = (\eta_1 + \eta_2)/G_1$ and $\lambda_2 = \eta_2/G_1$. This is consistent with the relaxation time spectrum found by Shaw *et al.* (350–2600 seconds) for a variety of naturally occurring biofilms.[1] Additionally, our relaxation time was much greater than that found by Hohne *et al.* (13.8 seconds) in compression.[13]

Effects of osmotic stress on the rheological properties

Elevated osmotic pressure of growth media is a known bacterial metabolic stressor that prompts a number of defensive changes by *S. epidermidis*, including increased export of EPS-related
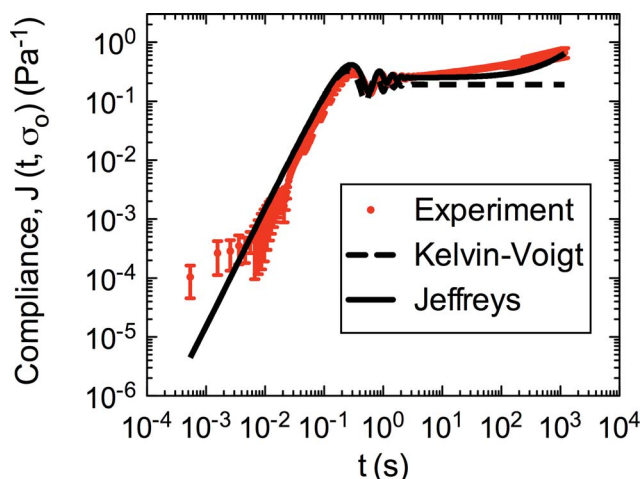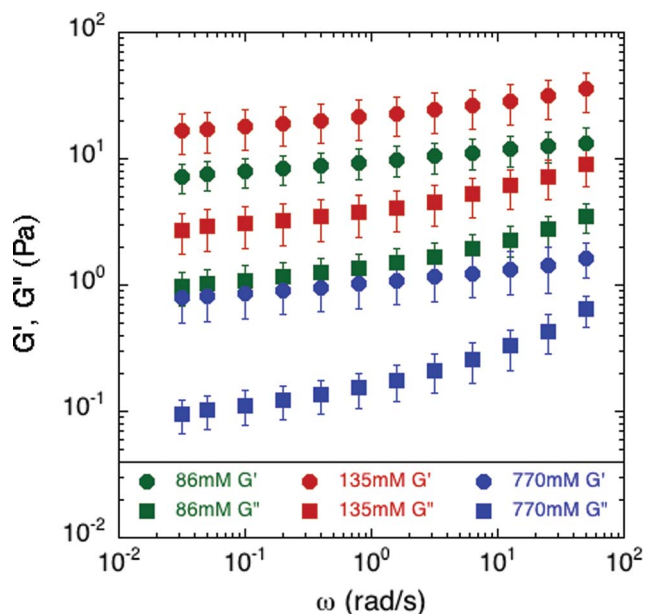
Fig. 7 Effect of [NaCl] on the elastic and viscous modulus of *S. epidermidis* biofilms. Error bars were plotted as the standard error of the mean, which includes 6 replicates of the physiological condition, 5 replicates of the no-salt-added condition, and 3 replicates of the high salt condition.

polysaccharides.[46,47] To probe the effects of osmotic stress on biofilm mechanical properties, the biofilms were grown in media of three different NaCl concentrations: 86 mM, 135 mM and 770 mM. By conducting small-amplitude oscillatory rheology, we determined that the concentration of NaCl affects the biofilm material properties. This is summarized in Fig. 7. The values of the moduli at a frequency of 1 Hz (6.283 rad per s) are displayed in Table 2 with the respective standard error of the mean.

At a frequency of 1 Hz, (selected for attention because of its biologically relevance as the fundamental frequency of human circulation) the biofilms grown with 86 mM NaCl had storage and loss moduli of 11.1 Pa and 1.9 Pa, respectively. However, high salt concentrations resulted in biofilms with significantly lower moduli, 1.2 Pa and 0.3 Pa for the elastic and viscous modulus, while human physiological salt conditions (corresponding to 135 mM in the figure and table) exhibited the highest moduli, 26.3 Pa and 5.2 Pa for the viscous modulus, respectively. Hence, there is a non-monotonic relationship between the magnitude of the moduli and the concentration of salt in the media.

We believe this trend can be explained by a combination of effects. The initial increase of moduli from the base condition to the human physiological condition may be due to increased

amounts of EPS, as salt is known to up-regulate genes responsible for EPS production.[46,47] This up-regulation would suggest that with higher salt concentrations, EPS concentrations continue to increase or level off after reaching a maximum rate of production. However, this effect cannot be the only one observed, because the moduli for the highest salt condition are significantly lower than the other conditions. Therefore, we suggest that after a certain concentration of salt is exceeded, an additional effect dominates.[48] One possible effect would be the screening of intermolecular Coulombic interactions that leads to destabilization of the biofilm matrix.[49] For example, sodium cation and chloride anion concentrations can disrupt interactions between the negatively charged *S. epidermidis* cells and the positively charged polymers, potentially causing them to dissociate or otherwise alter their configuration, thereby making the biofilm less elastic.

In order to ensure that our results were statistically significant and showed definitive changes between conditions, we conducted statistical analysis. We used mixed effects linear regression to determine if there was a relation between the values of the moduli to the various factors including: frequency, NaCl concentration, gap height, and whether measurements were done under tension or compression. The results are summarized in Table 3. Consistent with the prior discussion, the analysis suggested strong statistical associations between the modulus and the NaCl concentration (non-monotonic, with the highest values seen at concentrations mimicking human blood). Moreover, the analysis also found a statistically significance correlation of G' and G'' with gap height (higher modulus at lower gap height), and deformation history (higher modulus after compression) of the sample. The dependence on gap height and deformation history may be a signature that the biofilm experiences some irreversible change upon compression. Such irreversibility would be consistent with the behavior seen in creep testing, such as the yielding transition. This result would indicate that both the degree of pre-compression of the

Table 3 Statistical analysis of the effect of [NaCl], gap height, and deformation history on the moduli of *S. epidermidis* biofilm[a]

Elastic modulus

Feature	Fold change in G'	P value
[NaCl] 135 mM *vs.* 86 mM	2.2 (1.4, 3.4)	0.105
[NaCl] 770 mM *vs.* 86 mM	0.1 (0.1, 0.2)	0.002
Gap 250 μm *vs.* 300 μm	0.9 (0.8, 0.9)	0.036
Tension *vs.* compression	1.2 (1.1, 1.2)	0.023

Viscous modulus

Feature	Fold change in G''	P value
[NaCl] 135 mM *vs.* 86 mM	2.5 (1.6, 3.8)	0.051
[NaCl] 770 mM *vs.* 86 mM	0.1 (0.1, 0.2)	0.002
Gap 250 μm *vs.* 300 μm	0.7 (0.7, 0.7)	$<10^{-4}$
Tension *vs.* compression	1.0 (1.0, 1.0)	0.102

[a] Estimate (estimate −SE, estimate +SE).

Table 2 Effect of [NaCl] on moduli of *S. epidermidis* biofilm at 1 Hz. Values extracted from points in Fig. 7

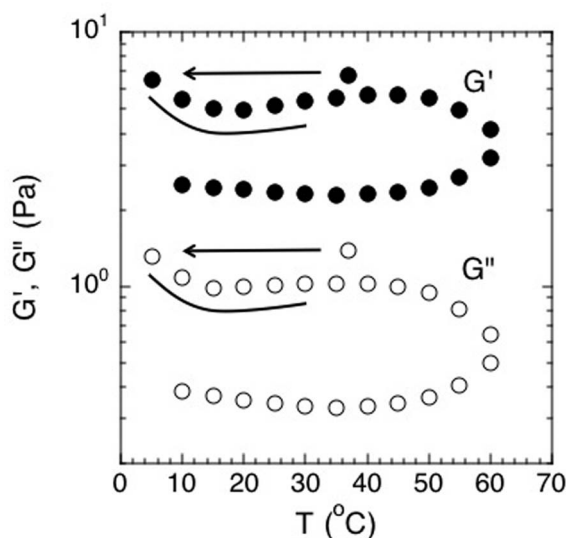|	86 mM	135 mM	770 mM
G'	11.1 ± 3.0 Pa	26.3 ± 9.1 Pa	1.2 ± 0.5 Pa
G''	1.9 ± 0.5 Pa	5.2 ± 1.8 Pa	0.3 ± 0.1 Pa

Fig. 8 Effect of temperature on the elastic and viscous moduli of *S. epidermidis* biofilms at a constant frequency of 1 Hz. Points were extracted from experiments conducted over a frequency range of 0.005–10 Hz. Order of experimentation was 37 °C, then 5 °C to 60 °C increasing at increments of 5, followed by decreasing from 60 °C to 10 °C in increments of 5. Data shown from 1 experiment for purposes of clarity.

biofilm, as well as the imposed pre-shear stress should be considered (and reported) when determining the mechanical properties of bacterial biofilms.

Temperature dependence of the rheological properties

To determine the effects of temperature on the linear rheological properties, we conducted small-amplitude oscillatory rheology at temperatures ranging from 5 °C to 60 °C. Here, temperature was increased and then decreased while the moduli were measured on a frequency range of 0.005–10 Hz. A number of conclusions can be drawn from the temperature dependence of the biofilm rheology.

First, the results show that time–temperature superposition is not valid for this material. The results are not consistent with the validity of time–temperature superposition in this material because the modulus does not display a monotonic dependence on temperature. Thus, measurements at a certain temperature and frequency cannot be uniquely shifted to match measurements at a lower temperature and frequency (data not shown). Consequently, the frequency range of the Fig. 4 viscoelastic moduli cannot be extended by means of this method.

Second, although time–temperature superposition is not valid, the results do display a very interesting hysteresis of the viscoelastic moduli with temperature. This effect is clearly apparent when plotted in Fig. 8 for both G' and G''. Here, the elastic and viscous moduli were plotted at the constant frequency of 1 Hz and plotted as function of temperature. The biofilm rheology is a strong function of temperature. The moduli reach a local maximum at around 45 °C and then drop when the temperature is increased further toward 60 °C. More importantly, the modulus does not return to its previous

condition upon cooling. This behavior shows that the environment it was previously exposed to affects the biofilm and its mechanical properties. We believe that the hysteresis can be due to the denaturing of linking molecules within the biofilm matrix at higher temperatures, thereby breaking EPS–cell associations or associations within the EPS itself. Rupture of these associations would act to reduce the modulus of the biofilm. An example of linking molecules would be denaturable proteins. These structures denature at higher temperatures and cannot return to their original shape after being cooled back down. Hence, the modulus would be irreversibly decreased after the biofilm undergoes a heating cycle.

Conclusion

We applied a range of rheological methods to interrogate *S. epidermidis* biofilms submerged in media. By adapting the rheometer to house a continuous-flow bioreactor, we eliminated the need to transport the biofilm from the growth environment and gained the ability to perform *in situ* rheology. This allowed us to study small-amplitude oscillatory rheology and creep rheology on materials that were previously inaccessible due to the fact that they had to be deformed or grown in non-physiological conditions. Using this method, we determined that *S. epidermidis* biofilms are soft, viscoelastic solids under linear deformation, but yield and show rheology that is similar to soft glassy materials and pastes upon non-linear deformation. The linear creep compliance was well modeled by the Jeffreys model because it incorporates a creep viscosity at long times. Additionally, we found that the biofilms display a non-monotonic trend upon an increase in osmotic stress and undergo hysteresis under changing temperatures. We believe that the critical temperature responsible for the onset of hysteresis should be examined further because this hysteresis may reveal features of temperature-dependent physical chemical interactions of the biofilm cells and matrix. The method reported in this paper can be simply adapted for other species and environmental conditions, thereby allowing *in situ* study that will lead to a more complete characterization of the rheological properties of these complex biomaterials.

Acknowledgements

References

1 T. Shaw, M. Winston, C. J. Rupp, I. Klapper and P. Stoodley, *Phys. Rev. Lett.*, 2004, **93**, 4.
2 R. M. Donlan and J. W. Costerton, *Clin. Microbiol. Rev.*, 2002, **15**, 167–193.
3 B. Rasmussen, *Nature*, 2000, **405**, 676–679.

4 L. Hall-Stoodley, J. W. Costerton and P. Stoodley, *Nat. Rev. Microbiol.*, 2004, **2**, 95–108.

5 K. K. Jefferson, *FEMS Microbiol. Lett.*, 2004, **236**, 163–173.

6 J. W. Costerton, P. S. Stewart and E. P. Greenberg, *Science*, 1999, **284**, 1318–1322.

7 H.-C. Flemming and J. Wingender, *Nat. Rev. Microbiol*, 2010, **8**, 623–633.

8 K. Cooksey and B. Wigglesworth-Cooksey, *Aquat. Microb. Ecol.*, 1995, **09**, 87–96.

9 W. G. Characklis, *Biotechnol. Bioeng.*, 1981, **23**, 1923–1960.

10 M. Otto, *Nat. Rev. Microbiol.*, 2009, **7**, 555–567.

11 H. M. Chung, M. M. Cartwright, D. M. Bortz, T. L. Jackson and J. G. Younger, *Shock*, 2008, **30**, 518–526.

12 M. M. Thornton, H. M. Chung-Esaki, C. B. Irvin, D. M. Bortz, M. J. Solomon and J. G. Younger, *J. Infect. Dis.*, 2012, **206**, 588–595.

13 D. N. Hohne, J. G. Younger and M. J. Solomon, *Langmuir*, 2009, **25**, 7743–7751.

14 B. W. Towler, C. J. Rupp, A. B. Cunningham and P. Stoodley, *Biofouling*, 2003, **19**, 279–285.

15 J. N. Wilking, T. E. Angelini, A. Seminara, M. P. Brenner and D. A. Weitz, *MRS Bull.*, 2011, **36**, 385–391.

16 A. Di Stefano, E. D'Aurizio, O. Trubiani, R. Grande, E. Di Campli, M. Di Giulio, S. Di Bartolomeo, P. Sozio, A. Iannitelli, A. Nostro and L. Cellini, *Microb. Biotechnol.*, 2009, **2**, 634–641.

17 W. L. Jones, M. P. Sutton, L. McKittrick and P. S. Stewart, *Biofouling*, 2011, **27**, 207–215.

18 S. Aggarwal, E. H. Poppele and R. M. Hozalski, *Biotechnol. Bioeng.*, 2010, **105**, 924–934.

19 S. Aggarwal and R. M. Hozalski, *Langmuir*, 2012, **28**, 2812–2816.

20 S. S. Branda, Å. Vik, L. Friedman and R. Kolter, *Trends Microbiol.*, 2005, **13**, 20–26.

21 R. L. Fournier, *Basic Transport Phenomena in Biomedical Engineering*, Taylor & Francis Group, New York, 2007.

22 K. M. Conlon, H. Humphreys and J. P. O'Gara, *J. Bacteriol.*, 2002, **184**, 4400–4408.

23 J. J. Boelens, J. Dankert, J. L. Murk, J. J. Weening, T. van der Poll, K. P. Dingemans, L. Koole, J. D. Laman and S. A. J. Zaat, *J. Infect. Dis.*, 2000, **181**, 1337–1349.

24 S. M. Finegold and E. E. Sweeney, *J. Bacteriol.*, 1961, **81**, 636–641.

25 J. Loscalzo and A. I. Schafer, *Thrombosis and Hemorrhage*, Williams & Wilkins, Baltimore, 1998.

26 S. P. Dzul, M. M. Thornton, D. N. Hohne, E. J. Stewart, A. A. Shah, D. M. Bortz, M. J. Solomon and J. G. Younger, *Appl. Environ. Microbiol.*, 2011, **77**, 1777–1782.

27 K. Miller, K. Chinzei, G. Orssengo and P. Bednarz, *J. Biomech. Eng.*, 2000, **33**, 1369–1376.

28 W.-C. Yeh, P.-C. Li, Y.-M. Jeng, H.-C. Hsu, P.-L. Kuo, M.-L. Li, P.-M. Yang and P. H. Lee, *Ultrasound Med. Biol.*, 2002, **28**, 467–474.

29 M. J. Paszek, N. Zahir, K. R. Johnson, J. N. Lakins, G. I. Rozenberg, A. Gefen, C. A. Reinhart-King, S. S. Margulies, M. Dembo, D. Boettiger, D. A. Hammer and V. M. Weaver, *Cancer Cell*, 2005, **8**, 241–254.

30 E. Linder-Ganz and A. Gefen, *J. Appl. Physiol.*, 2004, **96**, 2034–2049.

31 L. E. Freed, R. Langer, I. Martin, N. R. Pellis and G. Vunjak-Novakovic, *Proc. Natl. Acad. Sci. U. S. A.*, 1997, **94**, 13885–13890.

32 D. Bonn, P. Coussot, H. T. Huynh, F. Bertrand and G. Debrégeas, *Europhys. Lett.*, 2002, **59**, 786.

33 T. G. Mason and D. A. Weitz, *Phys. Rev. Lett.*, 1995, **74**, 1250.

34 G. Yin and M. J. Solomon, *J. Rheol.*, 2008, **52**, 785–800.

35 N. Koumakis and G. Petekidis, *Soft Matter*, 2011, **7**, 2456–2470.

36 G. M. Channell and C. F. Zukoski, *AIChE J.*, 1997, **43**, 1700–1708.

37 T. D. Brock and M. T. Madigan, *Biology of Microorganisms*, Prentice Hall, Englewood Cliffs, NJ, 1991.

38 J. W. Costerton, Z. Lewandowski, D. E. Caldwell, D. R. Korber and H. M. Lappin-Scott, *Annu. Rev. Microbiol.*, 1995, **49**, 711–745.

39 P. Stoodley, K. Sauer, D. G. Davies and J. W. Costerton, *Annu. Rev. Microbiol.*, 2002, **56**, 187–209.

40 P. H. T. Uhlherr, J. Guo, C. Tiu, X. M. Zhang, J. Z. Q. Zhou and T. N. Fang, *J. Non-Newtonian Fluid Mech.*, 2005, **125**, 101–119.

41 P. Coussot, *Soft Matter*, 2007, **3**, 528–540.

42 P. Coussot, H. Tabuteau, X. Chateau, L. Tocquer and G. Ovarlez, *J. Rheol.*, 2006, **50**, 975–994.

43 R. H. Ewoldt and G. H. McKinley, *Rheol. Bull.*, 2007, **76**, 4–6, 22–24.

44 C. Baravian and D. Quemada, *Rheol. Acta*, 1998, **37**, 223–233.

45 H. A. Barnes, J. F. Hutton and K. Walters, *An Introduction to Rheology*, Elsevier Science B. V., New York, 1989.

46 S. Rachid, K. Ohlsen, W. Witte, J. Hacker and W. Ziebuhr, *Antimicrob. Agents Chemother.*, 2000, **44**, 3357–3363.

47 Y. Lim, M. Jana, T. T. Luong and C. Y. Lee, *J. Bacteriol.*, 2004, **186**, 722–729.

48 P. C. Hiemenz and R. Rajagopalan, *Principles of Colloid and Surface Chemistry*, Taylor & Francis Group, New York, 1997.

49 H.-C. Flemming, J. Wingender, C. Mayer, V. Körstgens and W. Borchard, in *Cohesiveness in Biofilm Matrix Polymers*, ed. D. G. Allison, P. Gilbert, H. M. Lappin-Scott and M. Wilson, Cambridge University Press, 2000, pp. 87–106.